Journal of Luminescence 237 (2021) 118150

Contents lists available at ScienceDirect

Journal of Luminescence

journal homepage: www.elsevier.com/locate/jlumin

Exciton interaction with Ce^{3+} and Ce^{4+} ions in $(LuGd)_3(Ga,Al)_5O_{12}$ ceramics

Vasilii Khanin [a,*], Ivan Venevtsev [b], Kirill Chernenko [c], Vladimir Pankratov [c,d], Konstantin Klementiev [c], Thomas van Swieten [e], Arnoldus J. van Bunningen [e], Ivan Vrubel [f], Roman Shendrik [g], Cees Ronda [h], Piotr Rodnyi [b], Andries Meijerink [e]

[a] Delft University of Technology, Mekelweg 15, 2629 JB, Delft, the Netherlands
[b] Peter the Great St. Petersburg Polytechnic University, Polytechnicheskaya 29, 195251, St. Petersburg, Russia
[c] MAX IV Laboratory, Lund University, SE-22100, Lund, Sweden
[d] Institute of Solid State Physics, University of Latvia, 8 Kengaraga Iela, LV-1063, Riga, Latvia
[e] Utrecht University, Princetonplein 1, 3584 CC, the Netherlands
[f] Skolkovo Institute of Science and Technology, Moscow, 121205, Russia
[g] Vinogradov Institute of Geochemistry, Russian Academy of Sciences, Favorskogo 1A, 664033, Irkutsk, Russia
[h] Philips Research, High Tech Campus 4, 5656 AE, Eindhoven, the Netherlands

ARTICLE INFO

Keywords:
Garnet scintillators
Ce^{4+}
Excitons
Energy transfer
Synchrotron
XANES

ABSTRACT

Scintillators based on Ce-doped garnets are regularly co-doped with Mg^{2+} or Ca^{2+} to form Ce ions in 4+ state and reduce undesired afterglow. However overly high Ce^{4+} concentration leads to poor light yield performance. In order to understand the reason for variation in luminescence efficiency of Ce^{3+}- and Ce^{4+}-doped garnets we investigate the differences in energy conversion processes in complex $LuGd_2Ga_3Al_2O_{12}$:Ce^{3+}/Ce^{4+} ceramics by means of VUV synchrotron irradiation. At first we have established via transmission spectroscopy and X-ray absorption spectroscopy that $LuGd_2Ga_3Al_2O_{12}$:Ce, Mg sample contains cerium in the 4+ state only. Then we show with VUV spectroscopy efficient interaction of excitons with Gd^{3+} and Ce^{3+}, and lack of exciton absorption edge in $LuGd_2Ga_3Al_2O_{12}$:Ce^{4+} excitation spectrum. Instead, Ce^{4+} exhibits charge-transfer absorption band in the range of exciton emission. We suggest that when Ce^{4+} concentration becomes too high, the exciton → Gd^{3+} → Ce^{3+} energy transfer path is hindered. It leads to high intensity of Gd^{3+} luminescence in $Lu_1Gd_2Ga_3Al_2O_{12}$:Ce, Mg ceramics, but lowered Ce^{3+} X-ray excited luminescence. Fine balance between 3+ and 4+ Ce concentrations is necessary to achieve the best performance of garnet scintillators.

1. Introduction

Cerium doped complex garnets are actively investigated for scintillator [1] and persistent phosphor [2] applications. Modification of (Lu, Gd,Y)$_3$(Ga,Al)$_5$O$_{12}$:Ce^{3+} cation composition [3] allows fine-tuning of light yield, emission wavelength, level of afterglow, radiation absorption efficiency, luminescence temperature stability and etc. [4,5]. Adding small amounts of divalent ions like Mg^{2+} or Ca^{2+} can lead to lower levels of afterglow (by an order of magnitude) [6,7], and very fast (<50 ps) luminescence rise time under X-rays [8].

The improvement of timing characteristics of YAG:Ce, Mg [9] and LYSO:Ce, Mg [10] is ascribed to favorable change in charge migration processes by formation of Ce^{4+} (charge compensated with Mg^{2+}). A model of e-h interaction with Ce^{3+} and Ce^{4+} ions explains the extremely fast rise time kinetics [6] and low afterglow levels. The corresponding processes proceed as follows [11]:

$$Ce^{3+} + h \rightarrow Ce^{4+} \quad (1)$$

$$Ce^{4+} + e^{-} \rightarrow (Ce^{3+})^{*} \quad (2)$$

$$(Ce^{3+})^{*} \xrightarrow{\Delta t = 60\ ns} Ce^{3+} + h\upsilon \rightsquigarrow \quad (3)$$

According to processes (1)–(3), Ce^{3+} radiatively relaxes after two sequent events of capturing a hole (1) and afterwards an electron (2). The delay of electron capture by process (1) means that Ce^{3+} is not able to compete with electron traps for the initial volley of CB-electrons [12].

* Corresponding author.
E-mail address: khanin.vasilii@mail.ru (V. Khanin).

https://doi.org/10.1016/j.jlumin.2021.118150
Received 30 January 2021; Received in revised form 17 April 2021; Accepted 20 April 2021
Available online 3 May 2021

Contrary to Ce^{3+}, equilibrium Ce^{4+} (charge compensated) is available for immediate capture of electrons (2) directly leading to luminescence (3) [13]. Furthermore, Ce^{4+}, as Coulomb-active center in a 3+ lattice, provides efficient competition to electron traps [14]. Diminished amount of trapping then leads to increased light yield for LuAG:Ce, Mg [15]. Interestingly, increased light yield of LuAG:Ce, Mg is observed only for low concentrations of Mg co-doping. Likewise, in GGAG:Ce, Ca [16], GGAG:Ce, Mg [17,18] co-doping with Ca^{2+}, Mg^{2+} above 0.1% leads to lower light yield by factor of 1.3–2.

The model depicted above includes only e-h recombination on $Ce^{3+/4+}$ and does not account for excitons formation and their interactions with Ce and Gd ions. In garnets of simpler compositions, e.g. YAG exciton emission is detected as a broad UV emission band around 270 nm [19], while excitons distorted by antisite defects emit at around 300–350 nm [20]. The absorption bands of Ce^{3+} (4f-5d_2) overlap well with excitonic emission. Indeed, doping YAG with RE ions significantly distorts and quenches exciton emission (see e.g. Ref. [21] for Ce^{3+} or [22] for Pr^{3+}), indicating energy transfer to impurity RE ions.

In complex solid solutions of $(Gd,Y)_3(Al,Ga,Sc)_5O_{12}$ [23,24], the excitons emit at similar wavelengths of 250–350 nm, but with higher Gd^{3+} content their emission goes down in intensity. As such, in $Gd_3(Ga,Al)_5O_{12}$:Ce crystals no emission from excitons was detected so far, while excitation spectra of Gd^{3+} and Ce^{3+} still contained excitation peaks characteristic for excitons [25]. That can be attributed to complete energy transfer from excitons to Gd^{3+} ions.

Ce^{4+} also has an absorption band in the UV range due to charge transfer (CT) transition from the O^{2-} states of valence band to the Ce^{4+} ground state [13]. The CT absorption of Ce^{4+} does not lead to emission. Addition of Ce^{4+} potentially creates an exciton quenching channel (by CT absorption) that lowers the probability of exciton → Ce^{3+}/Gd^{3+} energy transfer. Thus we consider it important to study exciton interplay with Ce^{3+}, Ce^{4+} and Gd^{3+} ions in complex garnets.

In the current work we investigate the differences in energy migration processes in complex $Lu_3Ga_3Al_2O_{12}$ and $LuGd_2Ga_3Al_2O_{12}$ garnet ceramics doped with Ce^{3+} or Ce^{4+} ions. We first develop an understanding on broad band UV emission in $Lu_3Ga_3Al_2O_{12}$:Ce garnet ceramics and lack of it in Gd^{3+}-containing garnets. With X-ray Absorption Near Edge Structure (XANES) and transmission spectroscopy we establish that Mg^{2+} co-doping fully converts Ce to 4+ state in $LuGd_2Ga_3Al_2O_{12}$:Ce, Mg samples. Then we study the differences in excitation spectra of $LuGd_2Ga_3Al_2O_{12}$:Ce^{4+} and $LuGd_2Ga_3Al_2O_{12}$:Ce^{3+} luminescence in the 4.5–10 eV range under synchrotron irradiation.

1.1. Materials and experimental

Luminescence spectroscopy was conducted at photoluminescence endstation [26,27] of the FinEstBeAMS undulator beamline [28] of MAX IV synchrotron (Lund, Sweden) located at the 1.5 GeV storage ring. The range of utilized excitation energy for this work was 4.5–45 eV, while temperature was varied from 7 to 300 K. The excitation spectra were corrected for beamline photon flux by measuring a reference curve with AXUV-100G diode. In order to suppress high orders of the undulator excitation passing through the monochromator a set of the filters (SiO_2, MgF_2 and Al) were selected. Luminescence detection in UV–visible spectral range (200–800 nm) was performed by an Andor Shamrock (SR-303i) spectrometer equipped with 8259-01 Hamamatsu photon counting head. The emission spectra were corrected for the spectral sensitivity of the detection system.

XANES experiments were carried out on the Balder beamline [29] of MAX IV Laboratory (Lund, Sweden) located at the 3 GeV storage ring. The XANES spectra were measured in fluorescence detection mode by a 7-element silicon drift detector. Continuous energy scanning was performed at a speed ~3.5min/XANES. For each sample, 10 repeats were collected and afterwards accumulated into a resulting spectrum. The reference CeO_2 sample was measured in transmission mode in order to avoid self-absorption distortion.

Absorption spectra were recorded with a double-beam PerkinElmer Lambda 950 UV/vis/NIR spectrometer. The transparent ceramic samples were placed in one optical path of the deuterium/halogen lamp without placing a reference sample in the second path. The transmitted beams were detected by a PMT. Spectra were acquired with a resolution of 0.5 nm within a spectral range of 200–700 nm. Below 330 nm the deuterium lamp was used, which automatically switched to the halogen lamp above 330 nm.

X-ray excited luminescence spectra were measured under continuous X-ray (40 kV, 10 mA, 3 cm distance) excitation. Emission spectra were registered in a reflection geometry using a Lomo Photonica MDR-2 monochromator (0.3 nm resolution) coupled to a Hamamatsu H8259-01 photon counting head. The spectra were corrected for wavelength-dependent transmission of the monochromator and the spectral sensitivity of the PMT.

Ceramic $Lu_3Ga_3Al_2O_{12}$:Ce 0.2 mol.% and $Lu_1Gd_2Ga_3Al_2O_{12}$:Ce 0.2 mol.% garnet samples for this study were prepared at Philips Research Eindhoven by mixing the initial oxides Gd_2O_3, Lu_2O_3, Ga_2O_3, CeO_2 and Al_2O_3, purity no less than 99.99% (4 N), with a dispersing agent and distilled water. This slurry is then milled for 100 h on a roller bench in a plastic jar using 2 mm Al_2O_3 balls. After grinding, organic binders were added to the slurry, and the suspension was then dried in a drying chamber. The dried granulate was sieved using a metal sieve with a mesh size of <500 μm and then dry-pressed in a uniaxial press into 'green-body' pellets. After pressing, the resulting pellets were heat treated to burn off the organic binders. The pressed green-body pellets were then sintered for 8 h in an Astro Industries Inc. vacuum oven at a temperature of 1600–1750 °C, under high vacuum (10^{-5} to 10^{-6} mbar) or in oxygen atmosphere. The final ceramics are in the form of pills of 14 mm diameter and 1 mm thickness. Based on the X-ray diffraction patterns it was concluded that all samples consisted of a single garnet phase. One $Lu_1Gd_2Ga_3Al_2O_{12}$:Ce sample was co-doped 0.2 mol.% Mg. With transmission spectroscopy and XANES we established that the $LuGd_2Ga_3Al_2O_{12}$:Ce, Mg 0.2% sample had Ce in the 4+ state only, Fig. 1.

The XANES peak shape and Ce L_{III}-edge positions were compared for $LuGd_2Ga_3Al_2O_{12}$:Ce, $LuGd_2Ga_3Al_2O_{12}$:Ce, Mg and CeO_2 samples. The $LuGd_2Ga_3Al_2O_{12}$ singly doped with Ce exhibited an absorption peak at 5726 eV, showing dominant presence of Ce^{3+} [30]. The CeO_2 XANES profile showed two main peaks at 5731 and 5738 eV, caused by the interaction of hybridized 4f, 5d orbitals of Ce with O 2p orbitals of the nearest surrounding [31,32]. The XANES spectrum for $LuGd_2Ga_3Al_2O_{12}$:Ce, Mg repeated the one for CeO_2 suggesting complete conversion of Ce^{3+} to Ce^{4+} in Mg co-doped ceramics. From in-line absorption spectra, Fig. 1b, similar conclusion could be drawn. $LuGd_2Ga_3Al_2O_{12}$:Ce sample exhibited two absorption bands with maxima at 2.75 eV (450 nm) and 3.65 eV (340 nm) belonging to 4f-5$d_{1,2}$ spin and parity allowed transitions. After co-doping with large concentration of Mg, $LuGd_2Ga_3Al_2O_{12}$:Ce, Mg sample showed no 5d_1 absorption of Ce^{3+}, instead there was a strong CT absorption band of Ce^{4+} below 3.55 eV (350 nm) [13,33].

1.2. Results and discussion

1.2.1. Excitons, Ce^{3+} and Gd^{3+} excitation in mixed garnets

We first focus on emission of excitons, Gd^{3+} and Ce^{3+} and respective VUV excitation spectra to determine their interaction with each other. In Fig. 2a the emission spectra of $Lu_3Ga_3Al_2O_{12}$:Ce 0.2% and $LuGd_2Ga_3Al_2O_{12}$:Ce 0.2% samples under 6.4 eV excitation by synchrotron irradiation at 7 K are shown. The $Lu_3Ga_3Al_2O_{12}$:Ce 0.2% spectrum (orange curve) exhibits the double emission band of Ce^{3+} 5d-4f transitions at around 2.5 eV (500 nm) and the UV emission band at 4.6 eV (270 nm). The broad UV luminescence band in YAG and LuAG:Ce has been determined with optical and electron-paramagnetic resonance (EPR) methods as exciton related [19,21,34]. In similar solid solutions of e.g. $(Y,Lu)_3(Al,Ga)_5O_{12}$ [35], the excitons also emit at energies of 3.5–5 eV. For Gd-containing garnets the emission spectrum shows different features in the UV range. Instead of broad excitonic emission band the

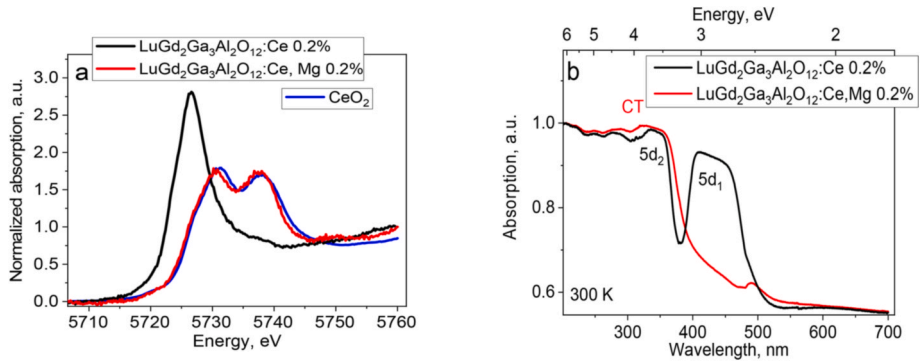

Fig. 1. a) XANES spectra performed at RT for $LuGd_2Ga_3Al_2O_{12}$:Ce and $LuGd_2Ga_3Al_2O_{12}$:Ce, Mg samples. For the reference CeO_2 measurement is shown. b) In-line transmission spectra for $LuGd_2Ga_3Al_2O_{12}$:Ce and $LuGd_2Ga_3Al_2O_{12}$:Ce, Mg measured at RT.

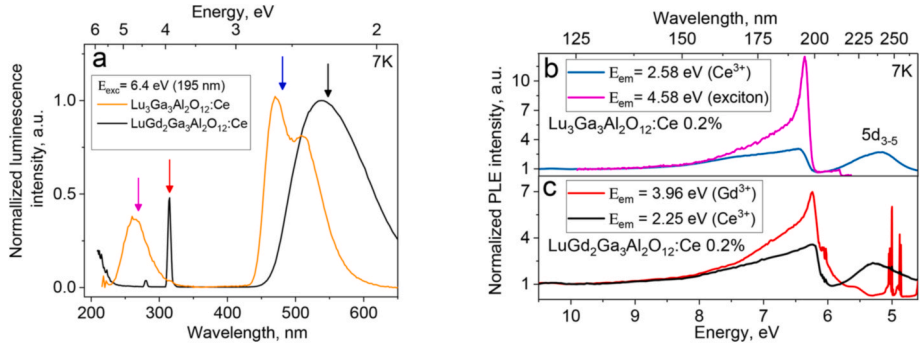

Fig. 2. a) Emission spectra of $Lu_3Ga_3Al_2O_{12}$:Ce 0.2% and $LuGd_2Ga_3Al_2O_{12}$:Ce 0.2% under 6.4 eV excitation at 7 K. The arrows indicate the monitored emission energy E_{em} for excitation spectra measurements in Fig. 2b and c b) Excitation spectra of UV emission band (4.58 eV, 270 nm) and Ce^{3+} (2.58 eV, 480 nm) in $Lu_3Ga_3Al_2O_{12}$:Ce 0.2% measured at 7K. c) Excitation spectra of Gd^{3+} (3.96 eV, 313 nm) and Ce^{3+} (2.25 eV, 550 nm) emission of $LuGd_2Ga_3Al_2O_{12}$:Ce 0.2% at 7K.

spectrum at 7 K is dominated by $^8S_{7/2} \rightarrow {}^6P_J$, $^8S_{7/2} \rightarrow {}^6I_J$ f-f transitions of Gd^{3+} 4.51 and 3.96 eV (275 and 313 nm, respectively) for $LuGd_2Ga_3Al_2O_{12}$:Ce 0.2%, black curve. It has been shown that excitonic emission can be distorted/quenched by the absorption bands of doped species (Ce^{3+} [21], Nd^{3+} [36], Pr^{3+} [22], Gd^{3+} [25,37]), which leads to exciton → dopant energy transfer. For temperature dependence of the $LuGd_2Ga_3Al_2O_{12}$:Ce 0.2% emission spectra and energy transfer between Gd^{3+} and Ce^{3+} please see supporting information.

Fig. 2b shows VUV excitation spectra of Ce^{3+} emission at 480 nm and of UV emission band at 4.58 eV (270 nm) in $Lu_3Ga_3Al_2O_{12}$:Ce 0.2%. Ce^{3+} spectrum exhibits a $5d_{3\text{-}5}$ ($^2D_{5/2}$, t_{2g} unresolved triplet state) excitation band [38] and the fundamental absorption edge that continues into the region of interband transitions (above ~7 eV, 180 nm). The 4.58 eV emission band is only excited effectively above 6.3 eV with a sharp excitation edge, which is a distinctive shape of excitation spectrum for excitons [39]. For more detail on the dependence of the excitation spectra of excitons on monitored emission wavelength please see supporting information.

In Fig. 2c the excitation spectra for Gd^{3+} and Ce^{3+} in $LuGd_2Ga_3Al_2O_{12}$:Ce 0.2% are shown. Gd^{3+} excitation spectrum exhibits several lines and a sharp absorption edge at 6.3 eV, while Ce^{3+} spectrum exhibits the same lines of Gd^{3+} transitions, the same absorption edge and an additional excitation band at 5.2 eV. The Gd^{3+} lines at 4.85 eV (255 nm), 5.02 eV (247 nm) and 6.05 eV (205 nm) are due to $^8S_{7/2} \rightarrow {}^6D_{9/2}$, $^8S_{7/2} \rightarrow {}^6D_{7/2}$ and $^8S_{7/2} \rightarrow {}^6G_J$ f-f transitions, respectively [40]. Existence of these lines in the excitation spectrum of Ce^{3+} indicates Gd^{3+}-Ce^{3+} energy transfer [41]. The 5.2 eV (240 nm) excitation band of Ce^{3+} belongs to $5d_{3\text{-}5}$ excitation band [42] (same as Fig. 2b, blue).

The excitation spectra of Ce^{3+} and Gd^{3+} emission in $LuGd_2Ga_3Al_2O_{12}$:Ce 0.2% from Fig. 2c indicate interaction between excitons and Ce^{3+}/Gd^{3+}. The sharpness of the absorption edge at 6.3 eV in both excitation spectra is due to exciton creation and its localization at Gd^{3+} or Ce^{3+} [21,43,44]. At 6.3 eV the contribution from excitons to Gd^{3+} is much more significant than to Ce^{3+}. That suggests a stronger interaction of excitons with Gd^{3+} instead of Ce^{3+}, most probably in view of Gd/Ce concentration ratio.

To summarise: Gd-free garnets show a UV emission band of significant intensity, the corresponding sharp excitation band at 6.3 eV allows to attribute the UV emission to formation of excitons. In garnets containing Gd^{3+} ($LuGd_2Ga_3Al_2O_{12}$:Ce) excitonic emission is quenched, while the excitation spectra of Gd^{3+} and Ce^{3+} still show the sharp excitation edge at 6.3 eV. That supports the notion that excitons transfer their energy to Gd^{3+} and Ce^{3+} ions.

1.2.2. *Ce^{3+} and Ce^{4+} excitation in mixed garnets*

Here we discuss luminescence and excitation spectra of $LuGd_2Ga_3Al_2O_{12}$:Ce, Mg under band-to-band excitation and their difference from those of $LuGd_2Ga_3Al_2O_{12}$:Ce. In Experimental we have shown with XANES and transmission spectroscopy that the Mg-codoped sample has no Ce^{3+}.

In Fig. 3a the emission spectra under 7 eV excitation of $LuGd_2Ga_3Al_2O_{12}$:Ce 0.2% (black) and $LuGd_2Ga_3Al_2O_{12}$:Ce, Mg 0.2% (red) are presented. The spectra show the same 2.25 eV Ce^{3+} emission and the lines of Gd^{3+} at 4.50 and 3.96 eV. The spectra are normalized on Gd^{3+} emission and $LuGd_2Ga_3Al_2O_{12}$:Ce, Mg exhibit three times lower Ce emission intensity probably due to lack of energy transfer between Gd^{3+} and Ce^{4+} as opposed to Gd^{3+} and Ce^{3+} interaction.

Excitation spectra of Ce luminescence in the two samples show very different properties, Fig. 3b. For $LuGd_2Ga_3Al_2O_{12}$:Ce sample excitation spectrum has been explained above (Fig. 2c, black): one can see the band at 5.2 eV (direct excitation of Ce^{3+}), Gd^{3+} lines at 4.85 and 5.02 eV ($Gd^{3+} \rightarrow Ce^{3+}$ energy transfer) and contribution from excitons as a sharp

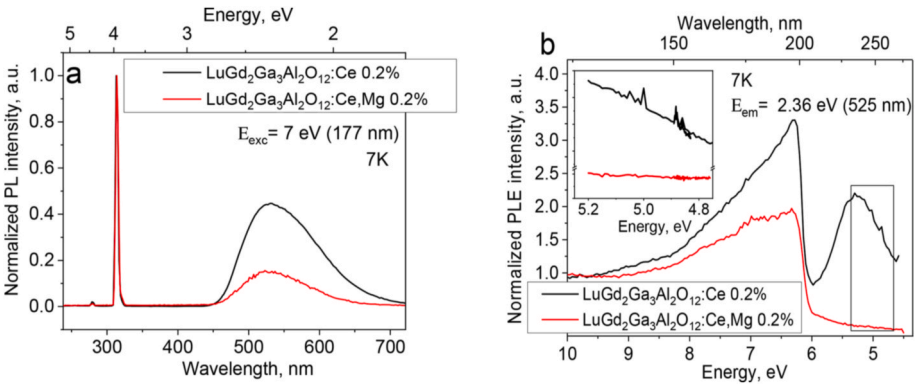

Fig. 3. a) Emission spectra at 7 K of $LuGd_2Ga_3Al_2O_{12}$ ceramics doped with 0.2% Ce (black) or 0.2% Ce and Mg (red), excited at 7 eV respectively. b) Excitation spectra at 7 K of Ce emission ($\lambda_{em} = 525$ nm) for $LuGd_2Ga_3Al_2O_{12}$ ceramics doped with 0.2% Ce (black) or 0.2% Ce and Mg (red). The inset shows the presence of Gd f-f transitions in $LuGd_2Ga_3Al_2O_{12}$:Ce excitation spectrum and lack of those in $LuGd_2Ga_3Al_2O_{12}$:Ce, Mg excitation spectrum.

edge at 6.3 eV. The excitation spectrum of $LuGd_2Ga_3Al_2O_{12}$:Ce, Mg sample shows no Gd^{3+} f-f transitions (see inset) and can only be excited above 6.3 eV. The shape of the band-to-band excitation is rather flat, showing small contribution from direct exciton formation [39]. From the difference between excitation spectra of $LuGd_2Ga_3Al_2O_{12}$:Ce and $LuGd_2Ga_3Al_2O_{12}$:Ce, Mg we propose that Ce^{4+} interacts neither with Gd^{3+} nor with excitons in ways that lead to luminescence.

Now we compare X-ray excited luminescence (XRL) spectra of the two $LuGd_2Ga_3Al_2O_{12}$:Ce and $LuGd_2Ga_3Al_2O_{12}$:Ce, Mg samples and their intensity, see Fig. 4. As with PL emission spectra, the shape of XRL emission spectra of the samples is the same: 2.25 eV band of Ce^{3+} 5d-4f transitions. The XRL intensity for $LuGd_2Ga_3Al_2O_{12}$:Ce, Mg 0.2% is lower by a factor of three, consistent with findings of W. Chewpraditkul et al. [17] on light yield of GGAG:Ce, Mg crystals with 0.1% Mg co-doping. We connect the low XRL intensity (low light yield) of garnets overly co-doped with Mg^{2+} to hindered exciton channel of energy transfer towards Ce ions. Formation of (Ce–Mg)-centers [45] and O^{-}-Mg^{2+} centers [6,14,46] was shown to occur, likely leading to lower scintillation efficiency. Additionally, the re-charging of Ce^{4+} to its equilibrium state can be delayed by hole-trapping [6,7] lowering the efficiency of Ce^{4+} as recombination center.

Based on the experiments described above we have constructed bandgap diagrams on how the thermalized charge carriers recombine on Ce for two extreme cases of only Ce^{3+} or Ce^{4+} present in garnets, Fig. 5a and b, respectively.

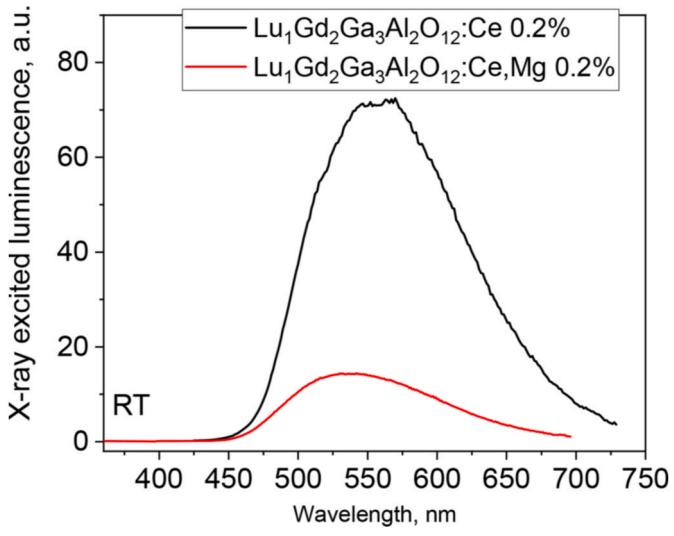

Fig. 4. X-ray excited luminescence spectra at 300K $LuGd_2Ga_3Al_2O_{12}$ ceramics doped with 0.2% Ce (black) or 0.2% Ce and Mg (red).

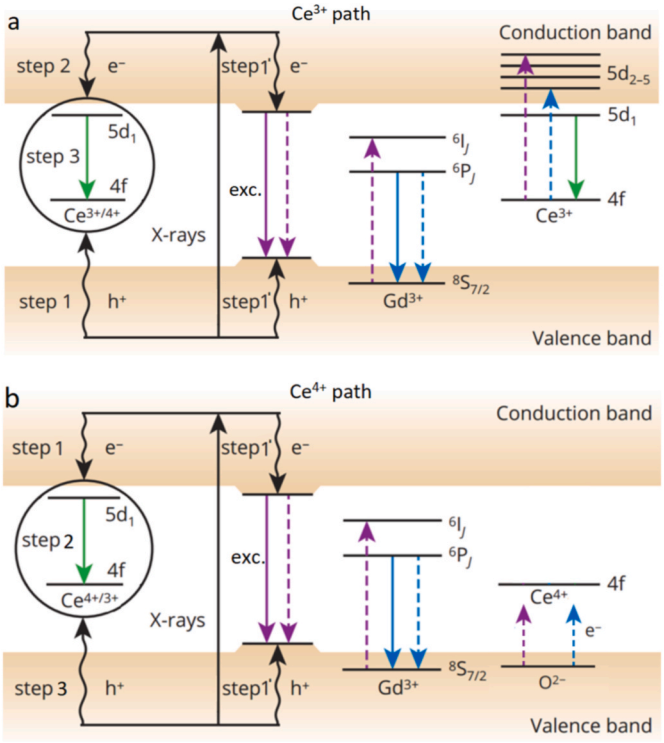

Fig. 5. Bandgap diagrams describing the mechanisms of e-h and exciton capture and transport towards a) Ce^{3+} and b) Ce^{4+}. 'X-rays' stands for creation of electrons (e^{-}) and holes (h^{+}) in CB and VB, respectively. The steps (1)–(3) of sequent e-h recombination on Ce^{3+} and Ce^{4+} are constructed after [14]. Step (1′) is an alternative path of exciton formation. Solid arrows indicate radiative transition: green – Ce^{3+} emission, purple – exciton emission, blue – Gd^{3+} 3.96 eV emission. Dashed arrows indicate resonant energy transfer or re-absorption. Note that in (b) excitonic path does not lead to Ce luminescence.

In the diagrams two recombination channels are described, the e-h (h-e) recombination on Ce, steps (1)–(3), and exciton formation, step 1′, with sequent energy transfer to Gd^{3+} and Ce^{3+}. After absorption of X-ray photon secondary electrons and holes thermalize to the bottom of CB and top of VB respectively. The e-h pair can be captured by Ce^{3+} or Ce^{4+} in sequent manner, leading to Ce^{3+} 5d-4f emission (green arrow). The e-h recombination on Ce^{4+} is usually distinguished from h-e recombination on Ce^{3+} experimentally with rise-time measurements [8] and transient spectroscopy [9]. In depth these mechanisms are describe in Refs. [12,14,16]. Here we are more focused on alternative process of

exciton formation (step 1'), which can then emit (solid purple arrow) or become localized/transfer energy to Gd^{3+} or Ce^{3+}states (dashed purple arrow). The Gd^{3+} $^8S_{7/2}\rightarrow{}^6I_J$ and Ce^{3+} $^2F_{5/2}/^2F_{7/2}\rightarrow{}^2D_{5/2}$ transitions overlap well with UV exciton emission [37]. Gd^{3+} can emit on its own as $^6P_J\rightarrow{}^8S_{7/2}$ at 3.96 eV (313 nm) as the last step for exciton path in $LuGd_2Ga_3Al_2O_{12}$:Ce, Mg sample (blue solid line, Fig. 5b), or Gd^{3+} can transfer energy to Ce^{3+} (Fig. 5a, for details see supporting information or [47]).

In $LuGd_2Ga_3Al_2O_{12}$:Ce case formation of excitons leads to Ce^{3+} luminescence, while Ce^{4+} in $LuGd_2Ga_3Al_2O_{12}$:Ce, Mg cannot interact positively with Gd^{3+} or excitons (dashed blue and solid arrow on CT in Fig. 5b). Additionally, CT absorption band of Ce^{4+} can re-absorb excitonic and Gd^{3+} emission further negatively impacting on the light yield of garnet materials.

Ce^{4+} in scintillators is used to rectify the short-comings of Ce^{3+} ability to compete with electron traps [7,12,48], but in case Ce^{4+} concentration becomes too high the number of transport pathways for delocalized charge to reach Ce is diminished.

2. Conclusions

Based on our finding we conclude the following. As Ce^{3+} $5d_{3\text{-}5}$ band is located in UV range where excitons emit, Ce^{3+} can accept energy from excitons. When part of the lattice is substituted with Gd ions, Ce^{3+} luminescence is enhanced via exciton → Gd^{3+} → Ce^{3+} energy transfer. The energy transfer from excitons is visible in excitation spectra for both Ce^{3+} and Gd^{3+}.

The excitation spectrum of $LuGd_2Ga_3Al_2O_{12}$:Ce, Mg (Ce^{4+}) luminescence shows no Gd^{3+} f-f transitions and no interactions with excitons. From the difference between excitation spectra of $LuGd_2Ga_3Al_2O_{12}$:Ce and $LuGd_2Ga_3Al_2O_{12}$:Ce, Mg we have found that Ce^{4+} interacts neither with Gd^{3+} nor with excitons in ways that lead to luminescence. The exciton → Gd^{3+} → Ce^{3+} energy transfer path is interrupted, which is one of the reasons for lowered Ce^{3+} X-ray excited luminescence in $LuGd_2Ga_3Al_2O_{12}$:Ce, Mg ceramics.

The combined presence of Ce^{3+} and Ce^{4+} ions allows efficient competition with hole and electron traps, as well as practical channels for host excitations to reach activator ions. Finely-tuned concentration of both Ce^{3+} and Ce^{4+} in the material has led to the highest light yield garnet materials.

Declaration of competing interest

The authors declare that they have no known competing financial interests or personal relationships that could have appeared to influence the work reported in this paper.

Acknowledgements

The authors acknowledge the expert help of the staff of MAX IV Laboratory. The research leading to this result has been supported by the project CALIPSOplus under the Grant Agreement 730872 from the EU Framework Programme for Research and Innovation HORIZON 2020. I. V. acknowledges the support of Russian Foundation for Basic Research # 20-52-S52001.

Appendix A. Supplementary data

Supplementary data to this article can be found online at https://doi.org/10.1016/j.jlumin.2021.118150.

References

[1] Y. Wang, G. Baldoni, W.H. Rhodes, C. Brecher, A. Shah, U. Shirwadkar, J. Glodo, N. Cherepy, S. Payne, Transparent garnet ceramic scintillators for gamma-ray detection, in: hard X-Ray, Gamma-Ray, Neutron Detect, Phys. XIV 8507 (2012) 850717, https://doi.org/10.1117/12.956437.

[2] J. Ueda, P. Dorenbos, A.J.J. Bos, K. Kuroishi, S. Tanabe, Control of electron transfer between Ce^{3+} and Cr^{3+} in the $Y_3Al_{5-x}Ga_xO_{12}$ host via conduction band engineering, J. Mater. Chem. C. 5642 (2015) 5642–5651.

[3] M. Fasoli, A. Vedda, M. Nikl, C. Jiang, B.P. Uberuaga, D.A. Andersson, K. J. McClellan, C.R. Stanek, Band-gap engineering for removing shallow traps in rare-earth $Lu_3Al_5O_{12}$ garnet scintillators using Ga^{3+} doping, Phys. Rev. B Condens. Matter 84 (2011), 081102.

[4] K. Kamada, T. Endo, K. Tsutumi, T. Yanagida, Y. Fujimoto, A. Fukabori, A. Yoshikawa, J. Pejchal, M. Nikl, Composition engineering in cerium-doped $(Lu,Gd)_3(Ga,Al)_5O_{12}$ single-crystal scintillators, Cryst. Growth Des. 11 (2011) 4484–4490.

[5] T. Kanai, M. Satoh, I. Miura, Characteristics of a nonstoichiometric $Gd_{3+\delta}(Al,Ga)_{5-\delta}O_{12}$: Ce garnet scintillator, J. Am. Ceram. Soc. 91 (2008) 456–462.

[6] C. Hu, S.P. Liu, M. Fasoli, A. Vedda, M. Nikl, X.Q. Feng, Y.B. Pan, ESR and TSL study of hole and electron traps in LuAG:Ce,Mg ceramic scintillator, Opt. Mater. (Amst) 45 (2015) 252–257, https://doi.org/10.1016/j.optmat.2015.03.049.

[7] M. Nikl, K. Kamada, V. Babin, J. Pejchal, K. Pilarova, E. Mihokova, A. Beitlerova, K. Bartosiewicz, S. Kurosawa, A. Yoshikawa, Defect engineering in Ce-doped aluminum garnet single crystal scintillators, Cryst. Growth Des. 14 (2014) 4827–4833.

[8] M.T. Lucchini, V. Babin, P. Bohacek, S. Gundacker, K. Kamada, M. Nikl, A. Petrosyan, A. Yoshikawa, E. Auffray, Effect of Mg^{2+} ions co-doping on timing performance and radiation tolerance of Cerium doped $Gd_3Al_2Ga_3O_{12}$ crystals, Nucl. Instruments Methods Phys. Res. Sect. A Accel. Spectrometers, Detect. Assoc. Equip. 816 (2016) 176–183, https://doi.org/10.1016/j.nima.2016.02.004.

[9] M.T. Lucchini, O. Buganov, E. Auffray, P. Bohacek, M. Korjik, D. Kozlov, S. Nargelas, M. Nikl, S. Tikhomirov, G. Tamulaitis, A. Vaitkevicius, K. Kamada, A. Yoshikawa, Measurement of non-equilibrium carriers dynamics in Ce-doped YAG, LuAG and GAGG crystals with and without Mg-codoping, J. Lumin. 194 (2018) 1–7, https://doi.org/10.1016/j.jlumin.2017.10.005.

[10] S. Blahuta, A. Bessière, B. Viana, P. Dorenbos, V. Ouspenski, Evidence and consequences of Ce4+ in LYSO:Ce,Ca and LYSO:Ce,Mg single crystals for medical imaging applications, IEEE Trans. Nucl. Sci. 60 (2013) 3134–3141, https://doi.org/10.1109/TNS.2013.2269700.

[11] A.J. Wojtowicz, A. Lempicki, D. Wisniewski, M. Balcerzyk, C. Brecher, The carrier capture and recombination processes in Ln^{3+}-activated scintillators, IEEE Trans. Nucl. Sci. 43 (3) (1996) 2168–2173, https://doi.org/10.1109/23.502312.

[12] V.M. Khanin, I.I. Vrubel, R.G. Polozkov, I.D. Venevtsev, P.A. Rodnyi, T. Tukhvatulina, K. Chernenko, W. Drozdowski, M.E. Witkowski, M. Makowski, E. V. Dorogin, N.V. Rudin, C. Ronda, H. Wieczorek, J. Boerekamp, S. Spoor, I. A. Shelykh, A. Meijerink, Complex garnets: microscopic parameters characterizing afterglow, J. Phys. Chem. C 123 (37) (2019) 22725–22734, https://doi.org/10.1021/acs.jpcc.9b05169.

[13] S. Liu, X. Feng, Z. Zhou, M. Nikl, Y. Shi, Y. Pan, Effect of Mg^{2+} co-doping on the scintillation performance of LuAG: Ce ceramics, Phys. Status Solidi Rapid Res. Lett. 8 (1) (2014) 105–109, https://doi.org/10.1002/pssr.201308199.

[14] M. Nikl, V. Babin, J. Pejchal, V.V. Laguta, M. Buryi, J.A. Mares, K. Kamada, S. Kurosawa, A. Yoshikawa, D. Panek, T. Parkman, P. Bruza, K. Mann, M. Muller, The stable Ce^{4+} center: a new tool to optimize Ce-doped oxide scintillators, IEEE Trans. Nucl. Sci. 63 (2) (2016) 433–438, https://doi.org/10.1109/TNS.2015.2495119.

[15] S. Liu, J.A. Mares, X. Feng, A. Vedda, M. Fasoli, Y. Shi, H. Kou, A. Beitlerova, L. Wu, C. D'Ambrosio, Y. Pan, M. Nikl, Towards bright and fast $Lu_3Al_5O_{12}$: Ce,Mg optical ceramics scintillators, Adv. Opt. Mater. 4 (5) (2016) 731–739, https://doi.org/10.1002/adom.201500691.

[16] Y. Wu, F. Meng, Q. Li, M. Koschan, C.L. Melcher, Role of Ce^{4+} in the scintillation mechanism of codoped $Gd_3Ga_3Al_2O_{12}$: Ce, Phys. Rev. Appl. 2 (2014) 44009.

[17] W. Chewpraditkul, N. Pattanaboonmee, O. Sakthong, K. Wantong, W. Chewpraditkul, A. Yoshikawa, K. Kamada, S. Kurosawa, T. Szczesniak, M. Moszynski, Scintillation properties of $Gd_3Al_2Ga_3O_{12}$: Ce, Li and $Gd_3Al_2Ga_3O_{12}$: Ce, Mg single crystal scintillators: a comparative study, Opt. Mater. (Amst). 92 (2019) 181–186.

[18] K. Kamada, M. Nikl, S. Kurosawa, A. Beitlerova, A. Nagura, Y. Shoji, J. Pejchal, Y. Ohashi, Y. Yokota, A. Yoshikawa, Alkali earth co-doping effects on luminescence and scintillation properties of Ce doped $Gd_3Al_2Ga_3O_{12}$ scintillator, Opt. Mater. (Amst). 41 (2015) 63–66.

[19] V. Murk, N. Yaroshevich, Exciton and recombination processes in YAG crystals, J. Phys. Condens. Matter 7 (29) (1995) 5857, https://doi.org/10.1088/0953-8984/7/29/012.

[20] Y. Zorenko, A. Voloshinovskii, V. Savchyn, T. Voznyak, M. Nikl, K. Nejezchleb, V. Mikhailin, V. Kolobanov, D. Spassky, Exciton and antisite defect-related luminescence in $Lu_3Al_5O_{12}$ and $Y_3Al_5O_{12}$ garnets, Phys. Status Solidi 244 (2007) 2180–2189.

[21] M. Kirm, A. Lushchik, C. Lushchik, G. Zimmerer, Investigation of luminescence properties of pure and Ce^{3+} doped $Y_3Al_5O_{12}$ crystals using VUV radiation, ECS Proc 99 (2000) 113–122.

[22] V. Gorbenko, A. Krasnikov, M. Nikl, S. Zazubovich, Y. Zorenko, Luminescence characteristics of LuAG:Pr and YAG:Pr single crystalline films, Opt. Mater. (Amst) 31 (12) (2009) 1805–1807, https://doi.org/10.1016/j.optmat.2008.11.030.

[23] T. Zorenko, V. Gorbenko, S. Witkiewicz-Lukaszek, Y. Zorenko, Luminescent properties of $(La,Lu,Gd)_3(Al,Sc,Ga)_5O_{12}$:Ce mixed garnets under synchrotron radiation excitation, J. Lumin. 199 (2018) 483–487, https://doi.org/10.1016/j.jlumin.2018.03.093.

[24] Y. Zorenko, V. Gorbenko, V. Savchyn, T. Zorenko, A. Fedorov, O. Sidletskiy, Development of scintillating screens based on the single crystalline films of Ce

doped (Gd,Y)$_3$(Al,Ga,Sc)$_5$O$_{12}$ multi-component garnets, J. Cryst. Growth 401 (2014) 532–536, https://doi.org/10.1016/j.jcrysgro.2014.01.075.
[25] A.P. Kozlova, V.M. Kasimova, O.A. Buzanov, K. Chernenko, K. Klementiev, V. Pankratov, Luminescence and vacuum ultraviolet excitation spectroscopy of cerium doped $Gd_3Ga_3Al_2O_{12}$ single crystalline scintillators under synchrotron radiation excitations, Results Phys 16 (2020) 103002, https://doi.org/10.1016/j.rinp.2020.103002.
[26] V. Pankratov, R. Pärna, M. Kirm, V. Nagirnyi, E. Nõmmiste, S. Omelkov, S. Vielhauer, K. Chernenko, L. Reisberg, P. Turunen, A. Kivimäki, E. Kukk, M. Valden, M. Huttula, Progress in development of a new luminescence setup at the FinEstBeAMS beamline of the MAX IV laboratory, Radiat. Meas. 121 (2019) 91–98, https://doi.org/10.1016/j.radmeas.2018.12.011.
[27] V. Pankratov, A. Kotlov, Luminescence spectroscopy under synchrotron radiation: from SUPERLUMI to FINESTLUMI, Nucl. Instrum. Methods Phys. Res. Sect. B Beam Interact. Mater. Atoms 474 (2020) 35–40, https://doi.org/10.1016/j.nimb.2020.04.015.
[28] R. Pärna, R. Sankari, E. Kukk, E. Nõmmiste, M. Valden, M. Lastusaari, K. Kooser, K. Kokko, M. Hirsimäki, S. Urpelainen, P. Turunen, A. Kivimäki, V. Pankratov, L. Reisberg, F. Hennies, H. Tarawneh, R. Nyholm, M. Huttula, FinEstBeaMS – a wide-range Finnish-Estonian beamline for materials science at the 1.5 GeV storage ring at the MAX IV laboratory, Nucl. Instruments Methods Phys. Res. Sect. A Accel. Spectrometers, Detect. Assoc. Equip. 859 (2017) 83–89, https://doi.org/10.1016/j.nima.2017.04.002.
[29] K. Klementiev, K. Norén, S. Carlson, K.G.V. Sigfridsson Clauss, I. Persson, The BALDER beamline at the MAX IV laboratory, J. Phys. Conf. Ser. 712 (1) (2016), 012023, https://doi.org/10.1088/1742-6596/712/1/012023.
[30] Y. Takahashi, H. Sakami, M. Nomura, Determination of the oxidation state of cerium in rocks by Ce L_{III}-edge X-ray absorption near-edge structure spectroscopy, Anal. Chim. Acta 468 (2002) 345–354.
[31] A.V. Soldatov, T.S. Ivanchenko, S. Della Longa, A. Kotani, Y. Iwamoto, A. Bianconi, Crystal-structure effects in the Ce $_{L3}$-edge x-ray-absorption spectrum of CeO_2: multiple-scattering resonances and many-body final states, Phys. Rev. B 50 (8) (1994) 5074, https://doi.org/10.1103/PhysRevB.50.5074.
[32] G. Kaindl, G. Schmiester, E.V. Sampathkumaran, P. Wachter, Pressure-induced changes in LIII x-ray-absorption near-edge structure of CeO_2 and CeF_4: relevance to 4f-electronic structure, Phys. Rev. B 38 (14) (1988) 10174, https://doi.org/10.1103/PhysRevB.38.10174.
[33] G. Dantelle, G. Boulon, Y. Guyot, D. Testemale, M. Guzik, S. Kurosawa, K. Kamada, A. Yoshikawa, Research on efficient fast scintillators: evidence and X-ray absorption near edge spectroscopy characterization of Ce^{4+} in Ce^{3+}, Mg^{2+}-Co-doped $Gd_3Al_2Ga_3O_{12}$ garnet crystal, Phys. Status Solidi Basic Res. 257 (8) (2020) 1900510, https://doi.org/10.1002/pssb.201900510.
[34] W. Hayes, M. Yamaga, D.J. Robbins, B. Cockayne, Optical detection of EPR of recombination centres in YAG, J. Phys. C Solid State Phys. 13 (1980) L1085.
[35] Y. Zorenko, V. Gorbenko, T. Zorenko, Y. Vasylkiv, Luminescent properties of the Sc^{3+} doped single crystalline films of (Y,Lu,La)$_3$(Al,Ga)$_5$O$_{12}$ multi-component garnets, Opt. Mater. (Amst) 36 (2014) 1760–1764, https://doi.org/10.1016/j.optmat.2014.03.028.
[36] A. Niklas, Thermoluminescence of YAG:Nd crystals coloured with x-rays, Appl. Phys. B Photophysics Laser Chem. 34 (2) (1984) 87–92, https://doi.org/10.1007/BF00697953.
[37] S.V. Nizhankovsky, A.Y. Dan'ko, Y.V. Zorenko, V.V. Baranov, L.A. Grin', V. F. Tkachenko, P.V. Mateichenko, Growth and the luminescence properties of a lutetium gadolinium garnet doped with Ce^{3+} and Pr^{3+} ions, Phys. Solid State 53 (1) (2011) 127–130, https://doi.org/10.1134/S1063783411010215.
[38] P. Dorenbos, Electronic structure and optical properties of the lanthanide activated RE_3 ($Al_{1-x}Ga_x$)$_5$O$_{12}$ (RE= Gd, Y, Lu) garnet compounds, J. Lumin. 134 (2013) 310–318.
[39] V. V Mikhailin, Synchrotron and undulator radiations and their applications in spectroscopy, Phys. Usp. 56 (4) (2013) 412–417, https://doi.org/10.3367/ufne.0183.201304i.0433.
[40] R.T. Wegh, A. Meijerink, R.J. Lamminmäki, Jorma hölsä, extending dieke's diagram, J. Lumin. 87 (2000) 1002–1004, https://doi.org/10.1016/S0022-2313(99)00506-2.
[41] T. Kushida, Energy transfer and cooperative optical transitions in rare-earth doped inorganic materials. I. Transition probability calculation, J. Phys. Soc. Japan. 34 (1973) 1318–1326.
[42] V.P. Dotsenko, I. V Berezovskaya, A.S. Voloshinovskii, B.I. Zadneprovski, N. P. Efryushina, Luminescence properties and electronic structure of Ce^{3+}-doped gadolinium aluminum garnet, Mater. Res. Bull. 64 (2015) 151–155.
[43] T. Tomiki, F. Fukudome, M. Kaminao, M. Fujisawa, Y. Tanahara, T. Futemma, Optical properties of YAG and YAP single crystals in VUV, J. Lumin. 40 (1988) 379–380, https://doi.org/10.1016/0022-2313(88)90242-6.
[44] Y. Zorenko, T. Voznyak, V. Gorbenko, E. Zych, S. Nizankovski, A. Dan'Ko, V. Puzikov, Luminescence properties of $Y_3Al_5O_{12}$:Ce nanoceramics, J. Lumin. 131 (1) (2011) 17–21, https://doi.org/10.1016/j.jlumin.2010.08.015.
[45] V. Babin, P. Herman, M. Kucera, M. Nikl, S. Zazubovich, Effect of Mg^{2+} co-doping on the photo- and thermally stimulated luminescence of the (Lu,Gd)$_3$(Ga,Al)$_5$O$_{12}$: Ce epitaxial films, J. Lumin. 215 (2019) 11608, https://doi.org/10.1016/j.jlumin.2019.116608.
[46] V. Laguta, M. Buryi, J. Pejchal, V. Babin, M. Nikl, Hole self-trapping in $Y_3Al_5O_{12}$ and $Lu_3Al_5O_{12}$ garnet crystals, Phys. Rev. Appl. 10 (3) (2018), 034058, https://doi.org/10.1103/PhysRevApplied.10.034058.
[47] K. Bartosiewicz, V. Babin, K. Kamada, A. Yoshikawa, M. Nikl, Energy migration processes in undoped and Ce-doped multicomponent garnet single crystal scintillators, J. Lumin. 166 (2015) 117–122, https://doi.org/10.1016/j.jlumin.2015.05.015.
[48] N.J. Cherepy, S.A. Payne, Z.M. Seeley, P.R. Beck, E.L. Swanberg, S.L. Hunter, in: Transparent Ceramic Garnet Scintillator Optimization via Composition and Co-doping for High-Energy Resolution Gamma Spectrometers (Conference Presentation), 2016, https://doi.org/10.1117/12.2237990.

Institute of Solid State Physics, University of Latvia as the Center of Excellence is supported through the Framework Program for European universities Union Horizon 2020, H2020-WIDESPREAD-01–2016–2017-TeamingPhase2 under Grant Agreement No. 739508, CAMART2 project.